A Silicon-Based, Three-Dimensional Neural Interface: Manufacturing Processes for an Intracortical Electrode Array

Patrick K. Campbell, Kelly E. Jones, Robert J. Huber, *Member, IEEE*, Kenneth W. Horch, *Member, IEEE*, and Richard A. Normann, *Member, IEEE*

Abstract—A method has been developed for the manufacture of a "three-dimensional" electrode array geometry for chronic intracortical stimulation. This silicon based array consists of a $4.2 \times 4.2 \times 0.12$ mm thick monocrystalline substrate, from which project 100 conductive, silicon needles sharpened to facilitate cortical penetration. Each needle is electrically isolated from the other needles, and is about 0.09 mm thick at its base and 1.5 mm long. The sharpened end of each needle is coated with platinum to facilitate charge transfer into neural tissue. The following manufacturing processes were used to create this array. 1) Thermomigration of 100 aluminum pads through an n-type silicon block. This creates trails of highly conductive p^+ silicon isolated from each other by opposing pn junctions. 2) A combination of mechanical and chemical micromachining which creates individual penetrating needles of the p^+ silicon trails. 3) Metal deposition to create active electrode areas and electrical contact pads. 4) Array encapsulation with polyimide. The geometrical, mechanical, and electrical properties of these arrays should make them well suited as interfaces to cortical tissue.

INTRODUCTION

IT has long been recognized that electrical stimulation of appropriate regions of sensory cortex evokes a perception in that particular sensory modality [18]. For example, electrical stimulation of the visual cortex evokes the perception of discrete points of light called phosphenes, while stimulation of the somatosensory cortex causes the sensation of touch. Furthermore, there is a topographic representation of each sensory modality over the appropriate region of sensory cortex. These observations have motivated research in sensory restoration via electrical stimulation of sensory cortex. One could implant an array of electrodes in an individual with a sensory deficit and stimulate specific sites on sensory cortex in order to recreate a limited sensory space.

Previous efforts to provide a limited sensory restoration of the visual system have centered on the use of planar

electrode arrays which were implanted upon the surface of the visual cortex [4], [8]. In order to elicit phosphenes, the electrodes in these arrays had to pass currents in the milliampere range. To maintain an acceptable current density on the electrode surface, these electrodes were required to have large surface areas (~ 1 mm^2). Another consideration in the design of these surface arrays was the need to minimize interactions between adjacent electrodes. Current from a surface electrode spreads into the cortex (basically a volume conductor) and summates with currents from adjacent electrodes if the interelectrode spacing is too small. The summated currents resulting from simultaneous current injections from two adjacent electrodes may excite a neuronal population which was not excited when current was injected through either electrode alone. Dobelle found that surface electrodes used to stimulate the visual cortex must have an interelectrode spacing greater than 2 mm, otherwise the phosphenes produced by the electrodes are indistinguishable from each other. This is presumably due to regions of stimulated tissue which overlap under the adjacent electrodes. In order for a visual prosthesis to be functional, it must contain a relatively large number of electrodes. If these electrodes are spaced 2 mm from each other, the resulting surface electrode array would cover a large portion of the occipital lobe. The electrode arrays produced by Brindley and Dobelle spanned many gyri. Thus, their phosphene maps were very discontinuous and bore only a rough correlation with the positions of the electrodes in their arrays. Due to this discontinuity, image resolution was found to be less than desired.

As a possible solution to this problem, it has been suggested that an array of electrodes with small surface areas, penetrating into the cortex, would require less current for threshold and would stimulate more localized regions of tissue [7], [22]. With more focal stimulation, the spacing between electrodes could be substantially decreased, and thus many electrodes could be placed within the same gyrus increasing the subject's sensory resolution. Implanting many electrodes within a single gyrus will eliminate the discontinuity produced by stimulation of multiple gyri.

We have previously described a silicon-based, three-dimensional array of penetrating electrodes which is

uniquely suited for cortical implantation [16], [17]. In this paper, we provide a complete description of these arrays and the manufacturing processes we have developed to create them. Because the electrode arrays are designed to be implanted into cat visual cortex, their dimensions were dictated by feline cortical structural characteristics. The implant is micromachined from silicon and contains an array of 100 penetrating electrodes, each of which will eventually be addressed with demultiplexing circuitry built into the device. Each electrode is a 1.5 mm long silicon needle coated with platinum at the sharpened end. These silicon needles are held together with a thin (~ 0.12 mm) substrate of silicon which is designed to float on the cortical surface. Each electrode is separated from neighboring electrodes with a 0.4 mm spacing. We feel that such an array can form the basic neural interface which may make direct electrical stimulation of cortical neurons a viable approach to providing sensory restoration.

MANUFACTURING METHODS

The starting material used in the manufacture of the arrays is a three inch diameter, 1.7 mm thick, 6–20 Ω-cm n-type $\langle 100 \rangle$ silicon wafer. A process known as thermomigration [3] is employed to create many trails of p^+ type silicon traveling from one side of the silicon wafer to the other. These p^+ trails are electrically isolated from each other by the resulting back to back pn junctions which are formed between any pair of p^+ trails. The silicon wafer is then subjected to a micromachining process which removes all but a thin layer of the n-type silicon surrounding each p^+ trail. The micromachining process sharpens the exposed p^+ trails into thin needles, and the end of each needle is coated with platinum. Electrical contact is made to the back side of a selected subset of silicon needles with thin, insulated gold wire. The entire array with the exception of the platinum needle tips is then insulated with polyimide and the leads are soldered into a percutaneous connector. Each of the manufacturing steps is explained in more detail below.

Thermomigration

The wafer, polished on one side, is coated on the polished side with a layer of aluminum (5 μm thick) in an electron-beam evaporator. The aluminum is then photolithographically patterned to create an array of aluminum squares, each measuring 325 μm on a side, and with a center-to-center spacing of 400 μm. The wafer is supported (with the patterned side down) by small quartz pins above a water-cooled plate and beneath a bank of quartz infrared lamps (Research Inc., Minneapolis, MN). At full power, the lamps heat the wafer to approximately 1250°C. With the lamps on one side, and the water-cooled plate on the other, a temperature gradient is created within the wafer. The aluminum squares form droplets of a silicon-aluminum eutectic which migrate along the temperature gradient towards the hotter side. As the eutectic droplets move through the wafer, the silicon, now doped to satu-

ration with aluminum, recrystallizes behind the droplets. Eventually the droplets traverse the entire thickness of the wafer, and deposit themselves on the hot surface. As aluminum is a p-type dopant, this process leaves a trail of p^+ type silicon in the n-type wafer. The thermomigration is accomplished in a matter of minutes. A schematic of the process can be seen in Fig. 1.

After thermomigration, both sides of the wafer are lapped and polished to remove the surface irregularities and any emergent bulk aluminum left by the thermomigration process. At this point, the silicon wafer is approximately 1.65 mm thick. Aluminum contact pads are created on one of the polished surfaces of the wafer so that there is one pad placed over each p^+ trail. The wafer is then cut into smaller dice for ease of handling during subsequent processes.

Creating the Three-Dimensional Structure

A computer controlled dicing saw (Micro Automation model 1006, Santa Clara, CA) is used to transform the thermomigrated wafer into a 10 × 10 array of rectangular columns by making deep orthogonal cuts into the silicon from the side opposite the aluminum pads. This is accomplished by mounting the silicon with the aluminum pad surface down, and sawing into the opposite surface using a diamond impregnated cuttting wheel rotating at 30 000 rpm. The mounted metal wheel used has a 0.25 mm blade thickness, 2 mm blade length and a 5 μm diamond grit size. The cuts made are 1.5 mm deep and are centered on the remaining n-regions between the thermomigrated p^+ trails. Eleven cuts indexed at 0.4 mm are made in one direction, the silicon block is rotated 90°, and eleven additional cuts are made with the same indexing. This sawing does not cut through the entire silicon block, but leaves a 0.15 mm thick substrate at the base of the cuts. Since the sawing is centered on the n regions between the p^+ trails, the sawing effectively creates from the trails, 100 individual silicon p^+ type square columns, having aspect ratios of approximately 10:1. These p^+ columns are separated from each other in the substrate by the remaining n-type silicon. As a consequence, the individual columns are electrically isolated from each other by a pair of opposing pn junctions. The sawing also leaves "fins" on the edge of the array along with "corner posts." These fins and corner posts are left in place at this time for subsequent processes. Fig. 2 shows a top view of the array after the sawing process. Fig. 3(a) is a side view showing the isolated p^+ columns, and (b) is a schematic of the electrical components created.

Chemical Etching to Refine Column Geometries

As a result of the sawing process, each one of the 100 square isolated p^+ columns is approximately 0.15 mm on a side, and 1.5 mm tall. These individual columns must next be chemically etched to a shape more suitable for eventual implantation. The etching of the square silicon columns is performed by a two step process. The first
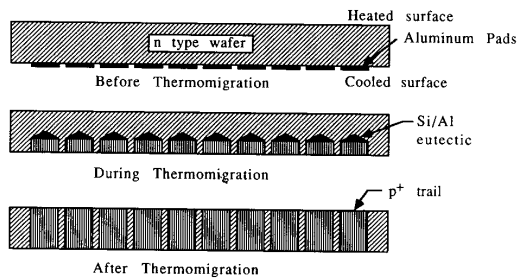
Fig. 1. Before the thermomigration process, aluminum pads are created on one side of an n-type silicon wafer. During the process a temperature gradient is applied to the silicon wafer which drives Si-Al eutectic droplets through the wafer. After the process, highly doped p$^+$ silicon trials result from the eutectic droplet passage through the n-type substrate.
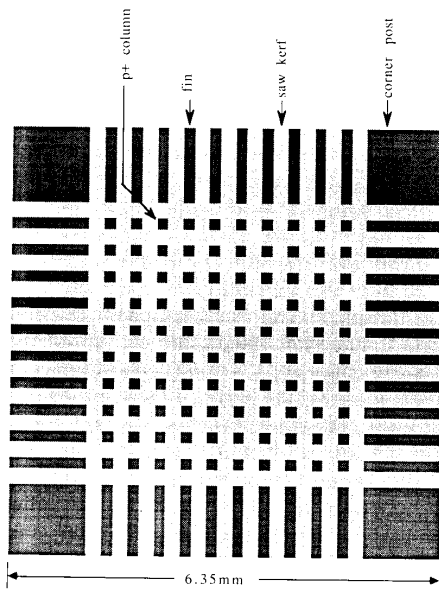

Fig. 2. Top view of array after using a dicing saw to make deep orthogonal cuts into the remaining n regions of the silicon wafer. The sawing produced high aspect ratio columns of p$^+$ silicon, along with fins and corner posts which are left in place for subsequent processes.

Fig. 3. Side view through the center of the array (a) showing isolated p$^+$ columns created by sawing with dicing saw. Also shown (b) is the equivalent circuit between two adjacent p$^+$ columns.

Fig. 4. For the dynamic etch, the array is (a) placed into a recessed Teflon holder to minimize lateral movement of etchant through the array, and (b) attached to a rotating clock motor and lowered into the acid so that the columns of the array are a short distance from the rotating stir bar.

etching step, called the "dynamic etch," isotropically etches the silicon throughout the entire structure by aggressively replenishing the etchant. The second etching step, called the "static etch," polishes and shapes the tops of the columns. Both steps use an isotropic etchant solution of 5% hydrofluoric and 95% nitric acid [21]. Various parameters of the described etching process may be changed to obtain a desired final column geometry. These geometries can range from extremely thin, flexible needles to a thicker, more rigid "missile" shape with a rounded or pointed top.

For the dynamic etch, a specially designed stirring system is used which flushes the etchant into the saw kerfs. As can be seen in Fig. 4(a), the array is placed in a recessed holder, so that the edges of the holder are even with the tops of the columns. This holder minimizes etch-
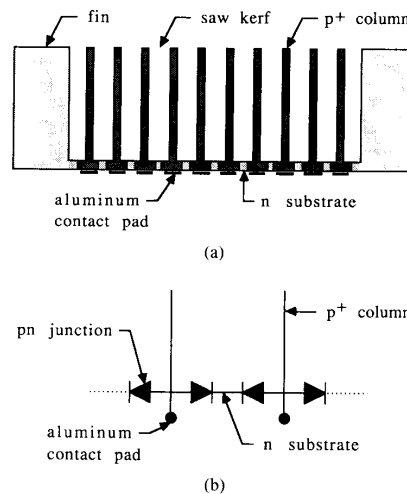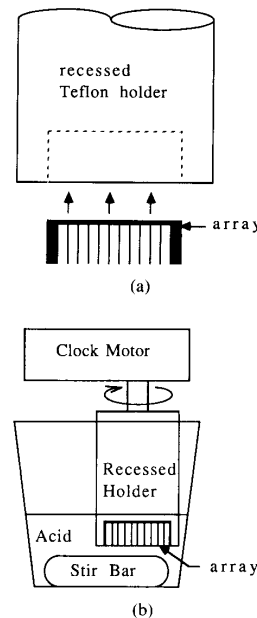
ing on the back side of the substrate, and prevents excess lateral etchant movement through the fins allowing for uniform array etching. The holder is attached to a 4 rpm clock motor, and lowered into the etchant until it is about 3 mm from a stir bar which is rotating at 375 rpm [Fig. 4(b)]. This combination of array and stir bar rotations greatly increases etching uniformity over the array sur-

face. Placing the array near the stir bar causes an aggressive and continuous flow of fresh etchant up into the saw kerfs. Etching is performed for a period of approximately 3 min. This process achieves three important shaping functions: it removes the saw damage from the sides of the columns and the kerfs, it reduces the column diameter, and it rounds the sharp edges at the base of each column reducing stress risers. These effects increase the mechanical strength of each column.

For the static etch, the array is left in the holder and placed in unstirred etchant with the columns pointing up. This etching is performed for a period of 3–5 min, depending on the desired final column tip shape. The static etch preferentially polishes and sharpens the tops of the columns, until the final column shape resembles a needle. The etch rate is greater at the tops of the columns because the activity of the etching solution at the base of the columns is reduced, and little fluid motion is present to replenish it. The final needle shape is about 0.09 mm on a side at the base and 1.5 mm tall. This two step etching process removes so much material that the final needle volume is only about 30% of the original column volume. With this needle shape and spacing, an array of needles displaces only about 2% of the cortical tissue in the volume penetrated by the array. Fig. 5(a)–(c) shows scanning electron micrographs of an array after the creation of columns with the dicing saw, after the dynamic etch and after the static etch, respectively.

Transforming Each Needle into an Active Electrode

Now that each p^+ needle is properly shaped and electrically isolated from its neighbors, it is necessary to coat each one with a substance which facilitates transfer of electrical charge from the p^+ silicon into neural tissue. Before this is performed, the fins and corner posts are removed with the use of a dicing saw. A thin metal foil is stretched over a thick silicon support block which contains deep, 0.25 mm thick grooves on 400 μm centers. The array is positioned on the foil (points down) so that each needle, when pushed through the foil, will enter into one of the grooves in the underlying support block. Using a micromanipulator, the array is pushed from the substrate side and the needles are driven through the metal foil so that the tips of the needles extend approximately 1.0 mm beyond the surface of the foil. The underlying grooved support block keeps the foil flat during this step, so that the distance of needle penetration will be approximately uniform over the array. The exposed needle tips extending through the metal foil are then briefly rinsed in 1 : 10 HF : H$_2$O to remove native silicon dioxide. An argon plasma sputtering system is then used to deposit a layer of gold onto the exposed needle tips, while the metal foil masks the region between the needles. This layer of gold serves to create an ohmic contact with the underlying silicon. After depositing the gold, platinum is then sputtered over the gold surface. After the deposition of the platinum is complete, the foil is removed, and the gold–
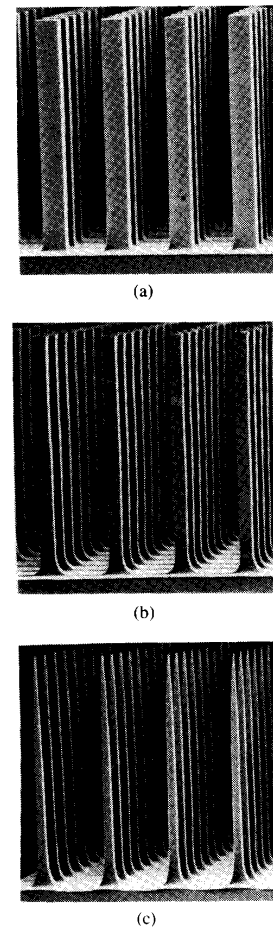
(a)

(b)

(c)

Fig. 5. Scanning electron micrographs show a side view of (a) the columns after creation by the dicing saw, (b) the columns after they have undergone the dynamic etch, and (c) the final needle geometry after the static etch. The center to center spacing between electrodes is 400 μm for scale.

platinum layers remaining on the needles are annealed to the silicon for 15 min at 400°C. Figs. 6(a) and (b) are scanning electron micrographs of a gold coated electrode tip, and an array showing the gold deposited on the silicon needles, respectively. The surface porosity seen in (a) is due to the sputtered gold, and not the silicon surface.

Making Contact to the Electrodes in the Array

Making electrical contact to each of the 100 electrodes in the array for current passage or recording in the cortex is a formidable task. We are currently developing demultiplexing VLSI circuitry which will allow analog current passage out any of the 100 electrodes with only five percutaneous leads. In the near future, this circuitry will be piggy-backed to the back side of the array using solder bump technology. Ultimately, it should be possible to have the circuitry built directly onto the rear surface of
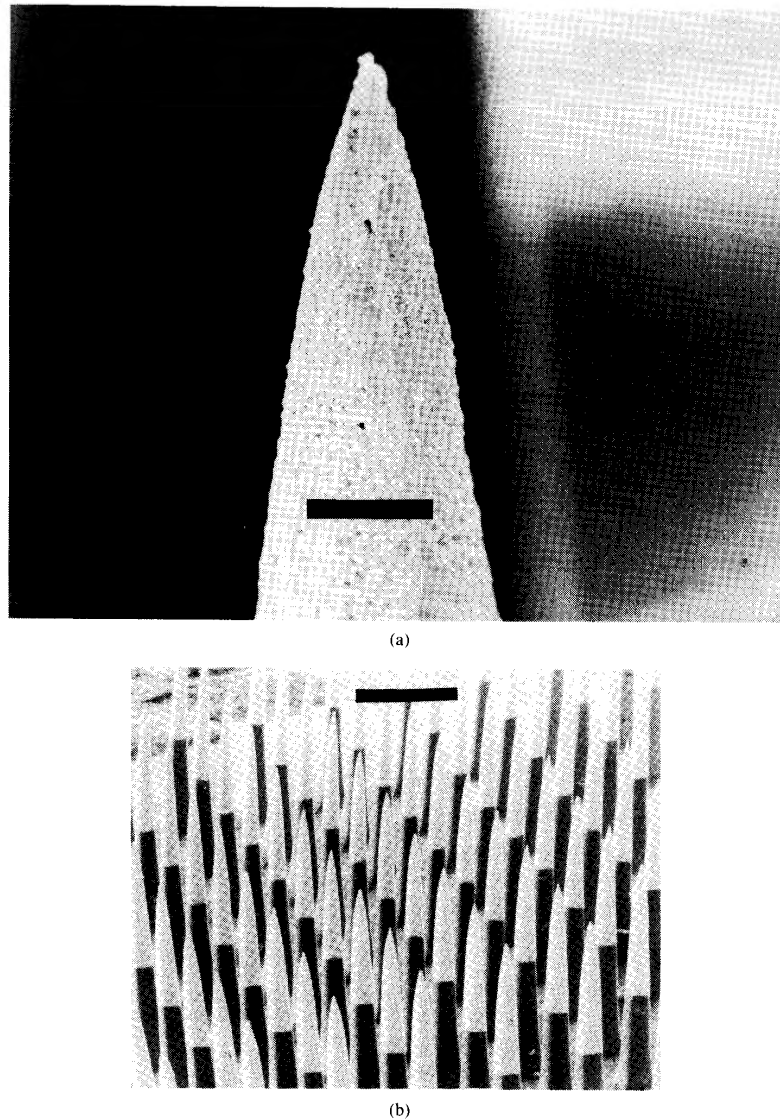
(a)

(b)

Fig. 6. Scanning electron micrographs of (a) the tip of a gold coated electrode, (scale bar is 15μm) and (b) an array showing gold deposited on the silicon needles (scale bar is 400 μm).

the array. Until we are able to take advantage of the demultiplexing circuitry, we are ultrasonically bonding 6 cm lengths of 37 μm diameter, polyimide insulated gold wire (California Fine Wire) onto selected aluminum pads on the back side of the array. Direct wire bonding to electrode pads has many practical limitations, such as the number of electrode leads which can easily be handled and the size of the resulting percutaneous connector.

Passivation of the Electrode Array

Thin film combinations of silicon oxide and silicon nitride have been used in the past as a passivation layer for implanted electronics. Much work is presently being directed towards the development of thin film passivation layers which are biocompatible and can withstand long implant periods in the body [9], [13]. Recently, it has been shown that polyimide provides long term protection of electronic circuitry when placed in 37°C saline if the proper primer (Hitachi PIQ Coupler-3) is used [14]. Polyimide reportedly forms a long term bond when cured onto the primed surface. Currently, we are insulating our electrode arrays using PIQ coupler and polyimide. The entire surface is dip coated with the PIQ coupler, which is subsequently cured at 350°C in air for 1 h. A small

drop of diluted polyimide (DuPont 2550) is placed on the back side of the array to secure the wire bond joints, which is subsequently partially cured in an oven. Using the same technique, additional layers of polyimide are then applied over the wire bond sites on the back of the array to ensure complete bonding site insulation. The rest of the structure (with the exception of the electrode tips) must now be insulated. The array is placed on a surface with the electrodes pointing up, and polyimide is flooded into the array, coating the entire surface. The polyimide is then wicked out of the kerfs, and baked for 1.5 h at 120°C. This polyimide application is repeated three times to ensure that there are no leakage paths resulting from pin holes. The polyimide layers are then fully cured at 200°C for 6 h. This process creates a thick layer of polyimide in the substrate between electrodes, and a much thinner layer on the electrode shanks. This thickness may be adjusted by varying the polyimide/solvent ratio and the number of coatings.

Using the same method as before, the points of the array are then pushed through another thin metal foil so that 0.5 mm of the tips extend above the foil surface. The polyimide on the points extending above the foil is then removed in an oxygen plasma. This exposes the underlying platinum and creates an electrode with a geometrical surface area of approximately 3.1×10^{-4} cm^2. The metal foil is then removed from the array. Finally, with the use of a variable temperature soldering iron, the loose ends of the lead wires are soldered into a percutaneous connector, along with a bare Pt–Ir reference electrode.

RESULTS

Manufacturing Uniformity and Repeatability

The manufacturing processes described herein are by no means finalized, and are constantly undergoing improvement. They require many individual steps and a great deal of handling which reduces yield and uniformity. However, it seems possible that process automation could greatly increase yields. Fig. 7(a) is a photograph of a completed electrode array and percutaneous connector. The array, as shown, could now be sterilized and implanted. Fig. 7(b) is a scanning electron micrograph of a completed array, showing six insulated gold leads arising from the back side of the substrate. The six leads make electrical contact to six electrodes located in the center of the array.

Since the geometrical characteristics of individual electrodes influence many of the electrical properties (impedance, capacitance, etc.) uniformity of electrode geometry over each array is important. Accordingly, the process we have developed has been designed to maximize geometrical uniformity. In an attempt to assess the micromachining process uniformity, arrays that had not undergone the thermomigration process were micromachined. We used n-type silicon so that variations in observed uniformity
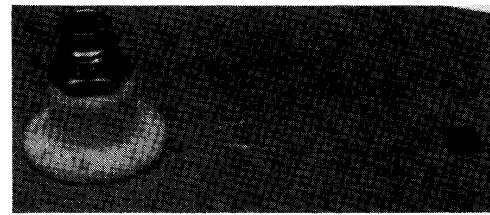
(a)
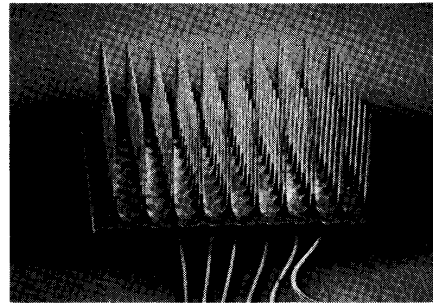
(b)

Fig. 7. (a) Photograph of completed array attached to percutaneous connector and (b) a scanning electron micrograph of completed array with polyimide insulation and showing six insulated gold lead wires. The center to center spacing between electrodes is 400 μm for scale.
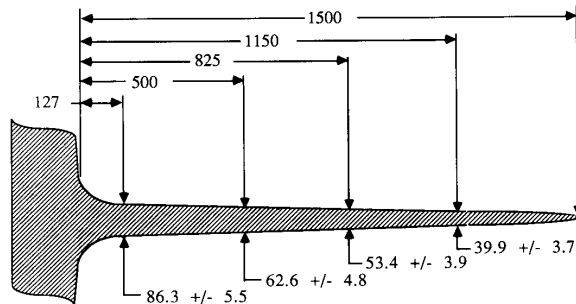

Fig. 8. A scaled drawing of an electrode side view showing the distance from the electrode bases at which all measurements were made. Listed is the average electrode diameter ± the standard deviation for 100 electrodes measured. All values listed are in micrometers.

would be solely due to the micromachining process, and not to differences in the p$^+$ and n-type silicon etch rate. Using a measuring technique with a 1 μm repeatability, all electrode diameters of a typical array were measured at four planes above the silicon substrate (127, 500, 825, and 1150 μm) [5]. Fig. 8 is an approximately scaled drawing of an electrode side view showing the four measurement planes, along with the average electrode diameters and the standard deviation of diameters (in microns) at those planes.

It was found that the corner electrodes had diameters 17% larger than the overall electrode diameter average,

while the center 64 electrodes exhibited a greater degree of uniformity. Thus, the standard deviations shown in Fig. 8 are largely due to the corner electrodes. This trend toward larger electrodes in the corners was consistently observed, and appears to result from a lack of uniform etchant flow in the two step wet etching process. Another cause of nonuniformity between electrodes made of thermomigrated silicon is the fact that n- and p^+ type silicon etch at different rates, particularly during the dynamic etch. If, due to misalignment, the columns are cut so that they contain some n-type silicon, undesirable electrode geometries result from the dynamic etch.

Mechanical Characteristics

While it might seem that these structures are extremely fragile, it has been found that they are remarkably strong and can easily withstand the forces associated with insertion into cortical tissue. Our initial efforts at implanting the arrays into cortical tissue using gentle mechanical force were unsuccessful due to incomplete electrode penetration. It was noted that the electrodes around the periphery of the array would be completely inserted into the cortex, while the electrodes located in the center of the array would only partially penetrate due to a substantial amount of cortical surface dimpling under the array. Subsequent attempts at implantation using high frequency, low amplitude vibration of the array were also unsuccessful for the same reasons. Ultimately, an impact insertion technique which produces high electrode array velocity has been found to achieve complete insertion of all electrodes in the array with a minimal amount of cortical deformation [23]. More than 70 implantations of these arrays into cortical tissue have been performed to date using this technique, and none of the electrodes in any of the arrays have been broken. The arrays have even proven strong enough to be implanted into cork stoppers using this technique. Using fine forceps, individual electrodes can be elastically deformed laterally to touch neighboring electrodes without breaking.

Electrical Characteristics

These electrode arrays consist of several different electrical components, such as the insulated lead wires, the pnp junction and needle resistance and capacitance, as well as the impedance of the platinum coated tip. Each of these components must be considered in order to predict how the array will function as a whole. Because of the difficulty in isolating and assessing the electrical characteristics of the individual array components in saline (such as the pnp junction resistance and capacitance), we have tested most of these components in room air. It is understood that a dry array will have different electrical characteristics than an implanted array, but an understanding of how the array functions when dry is required prior to predicting how it will operate once implanted.

A schematic of a single thermomigrated electrode on the edge of the array with the expected resistances, ca-
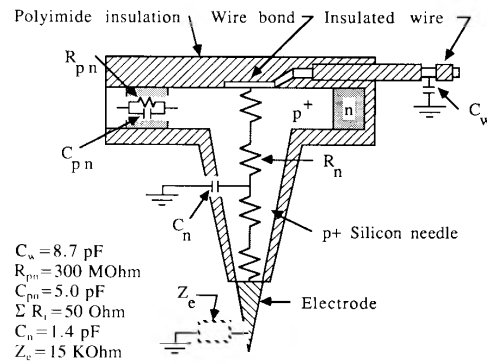

Fig. 9. A schematic of a thermomigrated electrode showing the expected resistances, capacitances and impedances when it is negatively biased. Included is the polyimide insulated wire capacitance (C_w), the pn junction capacitance (C_{pn}) and resistance (R_{pn}), the silicon needle resistance (R_n) and insulation capacitance (C_n), the electrode surface impedance (Z_e).

pacitances, and impedances is shown in Fig. 9. With each electrode separated from all the other electrodes by a region of n-type silicon, the leakage current between electrodes is limited to the back biased leakage of the pn junction formed around each electrode. The extent of this leakage was measured by placing probes from an I-V (current–voltage) tracer on a pair of aluminum pads over p^+ regions, and passing a 1 V, low frequency (1 Hz) ac signal through the pair of opposed pn junctions. The resulting leakage current was measured and displayed on an oscilloscope. In this configuration, for any given signal polarity, one of the junctions was forward biased (and thus contributed relatively insignificant impedance to any leakage current), and the other reverse biased. When the signal was of the opposite polarity, the other junction was reverse biased, and its leakage current could be measured. Using this technique, leakage current through each pn junction was measured for a set of arrays. Leakage currents (measured at 1 V) averaged 3.3 nA and ranged from 2 to 12.5 nA, corresponding to an average impedance of 300 MΩ (R_{pn} in Fig. 9). As expected, the back biased pn junction impedances were highly non-ohmic in nature. Break down voltage of the pn junctions was also assessed. Using the same technique with ac voltages up to 50 V, no pn junction break down was observed.

This technique was also used to determine the number of electrodes which were shorted together in the substrate. It has been found that adjacent p^+ regions can merge together during the thermomigration process, essentially shorting together adjacent electrodes. At this time, we are capable of making arrays with as few as 15% of the electrodes shorted to one or more neighbors.

The longitudinal impedance of the electrodes was also measured (ΣR_n). This was performed by painting the tips of the electrodes down to a metal surface using a highly conductive silver paint, and measuring the current flow resulting from a voltage applied between the aluminum pad on the back of the electrode and the metal surface. Of

the electrodes we measured, the average impedance was 46 ± 17 Ω. This impedance was measured at low ac frequencies, and was found to be ohmic in nature.

The capacitance of several components in the completed array was also measured. For the back biased pn junctions (C_{pn}), the capacitance was found to be 4.1 ± 0.4 pF at a 1 V bias, and 5.0 ± 0.6 pF at effectively no bias. The capacitance of the polyimide insulated gold wire in saline (C_w) was found to be 8.7 pF/cm, and the capacitance of the polyimide insulated portions of the electrode shank (C_n) has been calculated to be approximately 1.4 pF (assuming a 5 μm polyimide thickness, and 1000 μm of insulated needle shank). This value has been calculated at this time due to the difficulty in obtaining an accurate measurement.

Impedance of the electrode–electrolyte interface (Z_c) was also measured in saline at 1000 Hz. Individual electrodes were measured with respect to a Pt-Ir ground of large surface area. Preliminary results indicate that electrode impedances are in the 10–20 kΩ range.

DISCUSSION

Geometrical Considerations

There have been several attempts to produce arrays of either simulating or recording intracortical electrodes using standard silicon micromaching and photolithographic processes. Devices developed to date have generally been single penetrating silicon needles or comb-like structures with one or more electrodes positioned on the penetrating silicon tines [1], [10], [11], [15], [19], [20]. While these devices will provide useful interfaces to the nervous system in particular applications, they are not well suited for chronic cortical stimulation as a means of achieving sensory restoration because of the functional organization of sensory and motor cortex. Cortical structure is organized in such a way that adjacent regions of cortex represent adjacent regions of sensory space. Thus, the current injecting sites of an array of penetrating intracortical electrodes which is intended to provide limited restoration of a lost sense should be positioned in a two-dimensional grid within the same cortical lamina. One way in which the electrodes of the above mentioned comb-like structures could be positioned into the cortex would be to have many combs implanted side by side, with the tines of the comb structure penetrating into the cortex normal to the surface. If this method is used, such an array should be constructed so that the wire bonding/circuitry portion of the structure extends only a minimal distance above the cortical surface after implantation. This will help to avoid the problems associated with implant displacement due to movements of the brain with respect to the dura. Instead of implanting many tines normal to the cortical surface, one could implant a comb-like structure so that the tines travel just under and approximately parallel to the cortical surface. This would also create a two-dimensional grid of intracortical electrodes. However, it may prove difficult to get all of the electrodes within the same lamina using this technique, since few cortical regions are flat. This technique may be useful in presenting electrodes into cortical tissue buried within a sulcus.

We feel that the array geometry described briefly in previous reports [16], [17], and at length in this paper, is better suited for chronic intracortical stimulation for the restoration of a lost sense. With subtle changes (such as decreasing the exposed electrode surface area), the array should also be useful in recording cortical activity within the same lamina. The array can be easily implanted into the cortex, and the substrate which holds all of the electrodes together is very thin and "floats" on the cortical surface. The penetrating electrodes are strong enough to allow insertion into the cortex, while at the same time they are small in diameter so that only a minimal amount of cortical tissue is displaced upon implantation. By connecting the array to very flexible lead wires, movement of the brain with respect to the skull will not be transferred to the implanted array [6], [12].

As mentioned earlier, the manufacturing processes described herein are undergoing improvements and several of the steps merit further discussion.

Thermomigration

One key element to the manufacturing process described in this paper is thermomigration. Unfortunately, we have found it to be the least well behaved component in the process. A critical issue in the thermomigration process is the uniformity of the temperature gradient. Since the droplets follow the temperature gradient, if the gradient is not orthogonal to the silicon surface, neither will be the resulting p^+ trails. As these trails become the electrodes in subsequent manufacturing steps, it is important that the process produces orthogonal trails.

The geometry of our existing thermomigration oven tends to create a slightly hotter area in the center of the wafer, which gives the thermal gradient a lateral component. Various refinements to the basic process outlined above have allowed us to minimize but not eliminate this lateral component.

Another effect which complicates our thermomigration process is a seemingly random lateral wandering of the eutectic droplets as they traverse the wafer. This may be due to the phenomenon known as "random walk," described by Anthony and Cline [2], which is caused by defects in the crystal lattice of the silicon. Although the silicon wafers we are using have a dislocation density of less than $500/\text{cm}^2$, random walk is still a problem. One issue we have yet to resolve is the possibility that dislocations are being introduced into the silicon as a result of the stresses induced during our high temperature process.

Anthony and Cline described a method of minimizing random walk by thermomigrating with the thermal gradient slightly off from the $\langle 100 \rangle$ direction. We achieved this off axis gradient by applying a normal gradient to wafers cut 4° off of the $\langle 100 \rangle$ axis in the $\langle 010 \rangle$ direction.

However, we have not been able to eliminate the random walk problem. This phenomenon may be responsible for some of the electrode shorting problem mentioned earlier.

Another reason for the shorting problem is that some of the aluminum pads have a tendency to merge together before they migrate through the surface of the wafer. Once merged, the droplets migrate through the wafer as a single unit. This problem may be resolved by recessing the aluminum pads into the wafer prior to thermomigration.

It should be noted that changes in interelectrode spacing could greatly increase electrode array yield. For example, if the spacing between electrodes were increased to 600 μm, and the aluminum pad to be migrated increased to 400 μm, then a 200 μm spacing would exist between neighboring pads. From our experience, with a spacing of 200 μm between pads, there is very little chance that adjacent p$^+$ trails would merge together, and the proportion of nonshorted electrodes should increase significantly.

Electrical Properties

While the electrical properties of the array, as discussed above, are sufficient for producing a stimulating array, they are not ideal. One problem is in the nature of the pn junction formed. This junction is highly susceptible to leakage caused by surface contamination and surface residing charge carriers. In making the electrical measurements, it was necessary to treat the silicon surface to reduce this effect. To do so, the array (after being rinsed in acetone, alcohol, and DI water) was dipped briefly in the HF–HNO$_3$ etch (discussed previously) to remove the surface layer of silicon. It was then soaked for 20 min in concentrated HNO$_3$, forming a surface layer of silicon dioxide which protected the pn junction and decreased the current leakage by three orders of magnitude.

Since the interelectrode resistance of each array is highly dependent upon the surface cleanliness of the pn junction, the array insulation must be strongly bonded, and the array surface must be extremely clean and free of soluble substances prior to encapsulation. After encapsulating the arrays with polyimide, the interelectrode resistances dropped significantly indicating that more attention needs to be focused on this issue. Work is ongoing to develop improved cleaning processes, and possible underlying layers of thin film dielectrics, which when coupled with the polyimide encapsulation, should more effectively protect the junction in physiological environments.

Due to the electronic complexity of the array, there is some concern about how much of the current applied to a given electrode will actually pass out the metalized tip, and not be lost through other means. As can be seen in Fig. 9, most of the current applied to the lead wire of an electrode will pass out the metalized tip. Due to the capacitance of the lead wire, the pn junction and the insulated sections of the needle, the majority of the ac current that is lost will be due to this capacitance, with the losses largest at higher frequencies.

These losses will be small when the stimulating electrode is negatively biased. In this case, the electrode is electrically isolated from the rest of the substrate by the back biased pn junction immediately surrounding the electrode. Thus, only that surrounding pn junction will contribute to the total capacitance of the electrode. Thus, only that surrounding pn junction will contribute to the total capacitance of the electrode. However, ac current losses will increase when the electrode is positively biased. When this occurs, the pn junction surrounding the electrode is forward biased, and the electrode is essentially shorted to the n type silicon in the substrate between all the electrodes. Since the n-type silicon is coupled to the other 99 pn junctions in the substrate, the total capacitance of the stimulating electrode is increased substantially. Thus, the positive phases of a biphasic waveform will lose more current through the substrate due to capacitive effects than will the negative phase. This will lead to a nonbalanced charge passing out of the electrode tip, even if there was a balanced waveform sent to the electrode from the stimulus generating circuitry. This may necessitate the use of a monophasic stimulus signal linked to an exhausting circuit so that excess charge is not built up on the electrode surface.

Micromachining

The micromachining process described herein is unique in that it creates structures with very high aspect ratios, using equipment readily available in most semiconductor labs. The sawing process used to remove the n-type silicon between the p$^+$ trials produces a very high yield (100%) when using the intercut spacing and blade width mentioned previously. This spacing and blade width can easily be changed to produce columns of different spacing. We have found that while making these cuts with a 0.25 mm thick metal blade, the spacing between cuts can be reduced to 0.35 mm without breaking columns, resulting in columns that are 0.1 mm on a side.

We are currently investigating two methods to increase the uniformity of electrode diameters across the electrode array. First, since the diameter of the corner and edge electrodes of the array deviate the most from the average, this problem could be minimized by making a 12 × 12 array, and removing the outer edges to reveal a more uniform 10 × 10 array. Alternatively, the outer saw kerfs surrounding the 10 × 10 array could be made wider than normal to allow an increased flow of etchant around the corner and edge electrodes during the etching process. This should increase the etch rate of the corner and edge electrodes, and increase the overall electrode uniformity.

Implantations and Biocompatibility

There are many questions as to the effects of implanting this array into cortical tissue. Preliminary acute implantations in cats of passive arrays insulated with silicon nitride rather than polyimide indicate that after two months functional appearing neurons can be seen within 20 μm of

each electrode. There was also some evidence of resolved intracortical bleeding due to blood vessel damage which we believe resulted from the implantation. Work is ongoing to address the intracortical bleeding issue by determining the optimal impact insertion parameters, and to assess the biocompatibility of chronic implants in cats.

CONCLUSIONS

A method has been developed which allows fabrication of a "three-dimensional" array of 100 penetrating intracortical electrodes. The dimensions of the array have been chosen for use in cat cortex, but the manufacturing techniques are flexible enough to allow construction of arrays for a wide range of dimensions, or number of electrodes on the array. The overall array geometry is well suited for chronic implantation in cortex.

The impedance characteristics of these arrays have been measured and found to be well suited for stimulation of cortical tissue (very low impedance along the needle, very high impedance between electrodes). Some drawbacks do exist in the thermomigration method used to create these electrical characteristics. Often times electrodes are shorted together, and the nature of the isolating pn junction pairs is such that surface condition is critical to the effectiveness of the isolation. Also, the electrode tips should be coated with iridium oxide rather than platinum which will enhance the charge transfer capabilities of each electrode.

Although we are currently making arrays of 100 electrodes (and envision 1024 electrodes on a single array in the near future), we can electrically access only a few of the electrodes with our wire bonding technique. Work is underway to develop a demultiplexer chip which will be piggybacked directly to the array, enabling us to access all of the electrodes.

Chronic feline studies are ongoing to assess the insulative capabilities of the polyimide encapsulation, and overall array biocompatibility. Additional use of the array for stimulation and recording will determine the effectiveness of this structure for use as a functional neural interface.

REFERENCES

[1] D. J. Anderson, K. Najafi, S. J. Tanghe, D. A. Evans, K. L. Levy, J. F. Hetke, X. Xue, J. J. Zappia, and K. D. Wise, "Batch-fabricated thin-film electrodes for stimulation of the central auditory system," IEEE Trans. Biomed. Eng., vol. 36, pp. 693-704, 1989.

[2] T. R. Anthony and H. E. Cline, "Random walk of liquid droplets migrating in silicon," J. Appl. Phys., vol. 47, no. 6, pp. 2316-2324, 1976.

[3] ——, "Deep-diode arrays," J. Appl. Phys., vol. 47, no. 6, pp. 2550-2557, 1976.

[4] G. S. Brindley and W. S. Lewin, "The sensations produced by electrical stimulation of the visual cortex," J. Physiol., vol. 196, pp. 479-493, 1968.

[5] P. K. Campbell, K. E. Jones, and R. A. Normann, "A 100 electrode intracortical array: Structural variability," Biomed. Sci. Instr., vol. 26, pp. 161-166, 1990.

[6] P. K. Campbell, R. A. Normann, K. W. Horch, and S. S. Stensaas, "A chronic intracortical electrode array: Preliminary results," J. Biomed. Mater. Res. Appl. Biomat., vol. 23, no. A2, pp. 245-259, 1989.

[7] E. A. De Yoe, "An investigation in the awake macaque of the threshold for detection of electrical currents applied to striate cortex: Psychophysical properties and laminar differences," Ph.D. dissertation, Univ. Rochester, Rochester, NY, 1983.

[8] W. H. Dobelle and M. G. Mladejovsky, "Phosphenes produced by electrical stimulation of human occipital cortex, and their application to the development of a prosthesis for the blind," J. Physiol., vol. 243, pp. 553-576, 1974.

[9] D. J. Edell, "A peripheral nerve information transducer for amputees: Long-term multichannel recordings from rabbit peripheral nerves," IEEE Trans. Biomed. Eng., vol. BME-33, pp. 203-214, Feb. 1986.

[10] D. J. Edell, V. M. McNeil, and L. D. Clark, "Microfabrication technology for development of chronic neural information transducers," Proc. Internat. Electron Dev. Meet., 1986, pp. 180-183.

[11] H. Eichenbaum and M. Kuperstein, "Extracellular neural recording with multichannel microelectrodes," J. Electrophysiol. Tech., vol. 13, pp. 189-209, 1986.

[12] S. R. Goldstein and M. Salcman, "Mechanical factors in the design of chronic reading intracortical microelectrodes," IEEE Trans. Biomed. Eng., vol. BME-20, pp. 260-269, Apr. 1973.

[13] A. W. Hahn, "Innovative techniques for protective coatings of neural prosthetic devices. Material development and evaluation," 11th Quarterly Prog. Rep., NIH Contract No. N01-NS-4-2374, 1987.

[14] J. McHardy, D. I. Basiulis, G. Angsten, L. R. Higley, and R. N. Leyden, "Accelerated testing of polyimide coatings for neural prostheses. Polymeric materials for electronics packaging and interconnection," ACS Symp. Series, 407, pp. 168-175, 1989.

[15] H. D. Mercer and R. L. White, "Photolithographic fabrication and physiological performance of microelectrode arrays for neural stimulation," IEEE Trans. Biomed. Eng., vol. BME-25, pp. 494-500, June 1978.

[16] R. A. Normann, P. K. Campbell, and K. E. Jones, "A silicon-based electrode array for intracortical stimulation: Structure and electrical properties," in Proc. IEEE Eng. Med. Biol. Soc., vol. 11, pp. 939-940, 1989.

[17] R. A. Normann, P. K. Campbell, and W. P. Li, "Silicon-based microstructures suitable for intracortical electrical stimulation," in Proc. IEEE Eng. Med. Biol. Soc., vol. 10, pp. 714-715, 1988.

[18] W. Penfield and T. Rasmussen, The Cerebral Cortex of Man, New York: Macmillan, 1950.

[19] R. S. Pickard, "Printed circuit microelectrodes," TINS, pp. 259-261, Oct. 1979.

[20] O. J. Prohaska, F. Olcaytug, P. Pfundner, and H. Dragaun, "Thin-film multiple electrode probes: Possibilities and limitations," IEEE Trans. Biomed. Eng., vol. BME-33, pp. 223-229, Feb. 1986.

[21] H. Robbins and B. Schwartz, "Chemical etching of silicon," J. Electrochem. Soc., vol. 107, no. 2, pp. 108-111, 1960.

[22] S. F. Ronner and B. G. Lee, "Excitation of visual cortex neurons by local intracortical microstimulation," Exp. Neurol., vol. 81, pp. 376-395, 1983.

[23] P. J. Rousche and R. A. Normann, "A system for impact insertion of a 100 electrode array into cortical tissue," in Proc. IEEE Eng. Med. Biol. Soc., vol. 12, pp. 494-495, 1990.
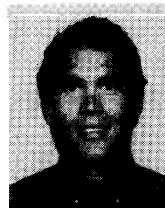
Patrick K. Campbell received the B.S. degree in mechanical engineering and the M.E. and Ph.D. degrees in bioengineering from the University of Utah, Salt Lake City.

From 1984 to 1986 he worked as a Development Engineer on the Ineraid Cochlear Implant at Symbion, Inc. Currently he is with Advanced Cardiovascular Systems, Santa Clara, CA. His research interests include neuroprosthetics, and methods of insulating electronic implants chronically implanted in the body.

Kelly E. Jones received the B.S.Ch.E. degree cum laude from the Ohio State University, Columbus, in 1985.

From 1985 to 1988 he worked as a Process/Product Development Engineer for the Technical Products Division of Corning Inc. He is currently pursuing the Ph.D. degree in bioengineering from the University of Utah, Salt Lake City, under a National Science Foundation Graduate Fellowship. His research centers on the creation of systems suitable for use in an artificial vision prosthesis.

Kenneth W. Horch (M'88) received the B.S. degree from Lehigh University, Bethlehem, PA, and the Ph.D. degree from Yale University, New Haven, CT.

He holds joint appointments as an Associate Professor of Physiology and Bioengineering at the University of Utah, Salt Lake City. His research interests are in the areas of sensory physiology, nerve repair and regeneration, and neuroprosthetics.

Robert J. Huber (M'69) received the B.S. and Ph.D. degrees in physics from the University of Utah, Salt Lake City.

After graduating he worked with nuclear reactor physics at Argonne National Laboratory. He joined the Microelectronic Division of General Instrument Corp. in 1966 and worked on MOS device physics. From 1971 through 1977 he was with the University of Utah Institute for Biomedical Engineering working on the neuroprosthesis program. He has been a faculty member of the Department of Electrical Engineering, University of Utah since 1977. His current research interests are silicon MOS device physics and solid state sensors and actuators.

Richard A. Normann (M'88) received the Bachelor's, Master's, and Doctor of Philosophy degrees from Berkeley campus of the University of California, Berkeley.

He joined the staff of the National Institutes of Health in 1974 and remained there until 1979 when he moved to the Department of Bioengineering. He also holds Research and Adjunct Professorships in the departments of Ophthalmology and Physiology in the School of Medicine at the University of Utah. His research interests are: information processing in the vertebrate retina and neuroprosthetics (creating interfaces to the nervous system).